Phase-field simulation of domain structures in epitaxial BiFeO3 films on vicinal substrates

B. Winchester, P. Wu, and L. Q. Chen

Related Articles

Additional information on Appl. Phys. Lett.

Journal Homepage: http://apl.aip.org/

Journal Information: http://apl.aip.org/about/about_the_journal

Top downloads: http://apl.aip.org/features/most_downloaded

Information for Authors: http://apl.aip.org/authors

Phase-field simulation of domain structures in epitaxial BiFeO₃ films on vicinal substrates

B. Winchester,[a] P. Wu, and L. Q. Chen

Department of Materials Science and Engineering, Pennsylvania State University, University Park, Pennsylvania 16802, USA

The ferroelectric domain structures of epitaxial BiFeO₃ thin films on miscut substrates were studied using a phase-field model. The effects of substrate vicinality towards (100) are considered by assuming charge-compensated surface and film/substrate interface. The predicted domain structures show remarkable agreement with existing experimental observations, including domain wall orientations and local topological domain configurations. The roles of elastic, electric, and gradient energies on the domain structures were analyzed. It is shown that the substrate strain anisotropy due to the miscut largely determines the domain variant selection and domain configurations. © *2011 American Institute of Physics*. [doi:10.1063/1.3605674]

Recently, there has been considerable interest in BiFeO₃ because of its coupled antiferromagnetic and ferroelectric order parameters,[1,2] high spontaneous polarization ($\sim$100 μC/cm²),[1–4] and high Curie temperature ($T_c = 850\,°C$), which make BiFeO₃ an attractive candidate for nanoelectronic applications.[5] BiFeO₃ has a rhombohedral perovskite structure with polarization along the $\langle 111 \rangle_c$ pseudocubic directions, leading to four ferroelastic variants and eight ferroelectric variants. Using the notation by Streiffer *et al.*,[6] we call the polarization variants $r_1^\pm = \pm [111]_c$, $r_2^\pm = \pm [\bar{1}11]_c$, $r_3^\pm = \pm [\bar{1}\bar{1}1]_c$, and $r_4^\pm = \pm [1\bar{1}1]_c$.

Domain wall orientations and domain structure strongly influence the ferroelectric properties of BiFeO₃ thin films. Domain walls can act as pinning sites that reduce remnant polarization,[7] while domain structure plays a role in ferroelectric fatigue. For instance, it has been shown that thin films consisting of only two polarization variants separated by 71° appear to have longer lifetimes than BiFeO₃ thin films with four variants.[7,8] Previous experimental work shows that substrate vicinality can influence the polarization symmetry; by depositing BiFeO₃ on a SrTiO₃ substrate miscut towards $(100)_c$, the number of preferred ferroelectric variants may be reduced from eight to two.[8–12] The domain structure changes from a mosaic pattern, consisting of mixed $\{101\}_c$ and $\{100\}_c$ domain walls, to a striped pattern with predominantly $\{101\}_c$-oriented walls. It has been suggested that the growth kinetics and substrate step morphologies may cause the reduced symmetry and variant selection.[8,12] However, the substrate miscut will also introduce anisotropy to the strain in a (001)-oriented BiFeO₃ film imposed by a (001)-oriented cubic substrate, which is otherwise isotropic. Therefore, we employ a phase-field method to explore the possibility that substrate strain anisotropy alone is sufficient to produce the observed domain variant selection.

We introduce two rectangular coordinate systems: a global system, with orthogonal axes x_i', with x_1' and x_2' in the plane of the film, and a local system based on the pseudocubic crystal cell, with axes x_i, where $x_2 = x_2'$, and x_1 and x_3 are related to x_1' and x_3' by a rotation about x_2' by the transformation $x_i' = a_{ij}x_j$ with transformation matrix given below in Eq. (2). The spatial polarization $\mathbf{P}' = [P_1'\ P_2'\ P_3']$ describes a domain structure with polarization components in the global axes. The temporal evolution of the polarization is determined by the time-dependent Ginzburg-Landau (TDGL) equation,

$$\frac{\partial P_i'(\mathbf{x}, t)}{\partial t} = -L \frac{\delta F}{\delta P_i'(\mathbf{x}, t)}, \qquad (1)$$

where F is the total free energy and L is a kinetic coefficient related to domain wall mobility. The free energy F is the sum of the Landau, gradient, elastic, and electrostatic energies. It should be noted that when we consider the elastic effect, we assume the film is coherent with the substrate, with misfit strains in the x_1'-x_2' plane of the film. The mathematical expressions for the Landau, elastic, electric, and gradient energies are described in Refs. 13–16, and the corresponding coefficients are listed in Ref. 21, as found in the literature.[17,18]

We consider a substrate miscut towards $[100]_c$. The transformation matrix corresponds to a counterclockwise rotation about the x_2' axis,

$$a_{miscut\_100} = \begin{pmatrix} \cos\theta & 0 & -\sin\theta \\ 0 & 1 & 0 \\ \sin\theta & 0 & \cos\theta \end{pmatrix}, \qquad (2)$$

where θ is the degree of rotation from the $[001]_c$ axis. We use a semi-implicit Fourier spectral method to solve Eq. (1).[14,15,19] We use a simulation size of $128\Delta x \times 128\Delta x \times 32\Delta x$ under periodic boundary conditions, with film and substrate thicknesses of both $14\Delta x$. The grid spacing Δx is related to the real value of the grid size through the domain wall energy: we choose $\Delta x = \frac{1}{2}l_0$, where $l_0 = \sqrt{G_{110}/\alpha_0}$, using gradient energy coefficients of $G_{11}/G_{110} = 0.3$ and $G_{44}/G_{110} = G m_{44}/G_{110} = 0.15$. If l_0 is 2.0 nm, then G_{11} corresponds to 4.73×10^{-10} C⁻²m⁴N, and the domain wall

[a] Author to whom correspondence should be addressed. Electronic mail: bmw200@psu.edu.

energy density is about 0.10 Jm^{-2} for 71° domain walls. We assumed an isotropic background dielectric constant of 50, a temperature of T = 298 K and a time step of $\Delta t/t_0 = 0.08$.

We start the simulation with small random polarization values. We set the initial P_3 to be positive, since existing experimental observations show that the direction of the P_3 polarization component for all variants are all out-of-plane due to a small built-in voltage resulting from the difference between the film surface and the film/substrate interface. We employ short-circuit electric boundary conditions on both film surfaces.

We compare an $(001)_c$-oriented film and a film with 4° miscut towards $[\bar{1}00]$, with the bi-axial strain of a coherent BiFeO$_3$ film on a SrTiO$_3$ substrate, $\varepsilon'_{11} = \varepsilon'_{22} = -1.5\%$. In good agreement with experiment,[8,20] the $(001)_c$-oriented film has all four ferroelastic variants present, while the miscut film has broken polarization symmetry, i.e., preferring only two ferroelastic variants, r_1 and r_4, as shown in Fig. (1). The polarizations within these two variants are related by 71° and they form striped domain patterns with domain walls along $(101)_c$. The $(001)_c$-oriented film contains all four ferroelastic variants in a mosaic pattern, with a mixture of 71° and 109° domain walls in the expected $\{101\}_c$ and $\{100\}_c$ domain wall orientations.[6] It should be noted that the only difference between the simulation conditions for the $(001)_c$-oriented film and the miscut film is the direction of the biaxial strain with respect to the film. It has been previously suggested that the formation of two variant domain structures might be due to the presence of surface ledges during film growth. The present simulation results demonstrate an alternative mechanism for the formation of two-variant domain structures in a miscut thin film.

To better understand the mechanism for the polarization variant selection, we analyzed the effect of various energetic contributions by deliberately eliminating one or more of them, i.e., we conducted phase-field simulations of domain structure formation in a BiFeO$_3$ film grown on a miscut substrate by excluding either the electric energy or the elastic energy, or both. As expected, we found that when both elastic and electric energy are excluded, all polarization domains are degenerate, i.e., all ferroelastic variants are equally favored [Fig. 2(d)]. This follows from the fact that the Landau and gradient energies are degenerate and isotropic for all ferroelectric variants and do not vary with film orientation. Likewise, including the electric energy alone has a little effect on the variant degeneracy [Fig. 2(b)]. It is noted that excluding the elastic energy contribution leads to vertical domain walls, which minimizes the domain wall energy relative to tilted domain walls, which are typically due to elastic strain energy minimization [Figs. 2(b) and 2(d)].

When elastic energy is included, the substrate miscut has a marked effect on the polarization variant selection. The film retains the experimentally-observed r_1 and r_4 striped domain pattern, as seen in Fig. 2(a). Excluding just the electrostatic interactions has a little effect on the two-variant striped domain patterns [Fig. 2(c)].

The elastic strain energy effect can be understood by examining the local strains, imposed from the global strains under the standard second-rank tensor transformation, $\varepsilon = a\varepsilon'a^{-1}$. The relevant term here is the shear strain along the miscut direction, $\varepsilon_{13} = (-\varepsilon'_{11} + \varepsilon'_{33})\cos\theta\sin\theta$, which indicates that the global strains contribute to a non-zero local ε_{13}. This ε_{13} term is negative for compressive global in-plane strains and positive for tensile strains. Thus, under sufficiently large ε'_{11}, two polarization variants will be favored to relax the elastic energy: r_1 and r_4 for compressive strains or r_2 and r_3 for tensile strains (Fig. 3).

To test this, we examined the effect of varying strains on the miscut film, once again including all the energy terms. The results, presented in Figure 4, support this hypothesis,

FIG. 1. (Color online) PFM-style images of simulation of (a) $(001)_p$-oriented BiFeO$_3$ and (c) miscut BiFeO$_3$. PFM images of (b) $(001)_c$-oriented BiFeO$_3$ and (d) miscut BiFeO$_3$. In (a) and (b), there is a mixture of all four ferroelastic variants. The white regions represent two in-plane variants (r_1 and r_4), while the lightly- and darkly-colored regions represent the r_2 and r_3 variants, respectively. In the images of miscut films, (c) and (d), the dark- and light-striped regions are mixed r_1/r_4 domains with 71° domain walls. (Figs. 1(b) and 1(d) reprinted with permission from Jang et al.[20])

FIG. 2. (Color online) Domain structures of miscut BiFeO$_3$ under different energy conditions: (a) with all energy forms included, (b) with electric but not elastic energy, (c) with elastic but not electric energy, and (d) with neither elastic nor electric energy. The elastic energy drives the symmetry non-degeneracy, and only the simulations which include elastic energy term, (a) and (c), form striped domain structures consisting of only two variants.
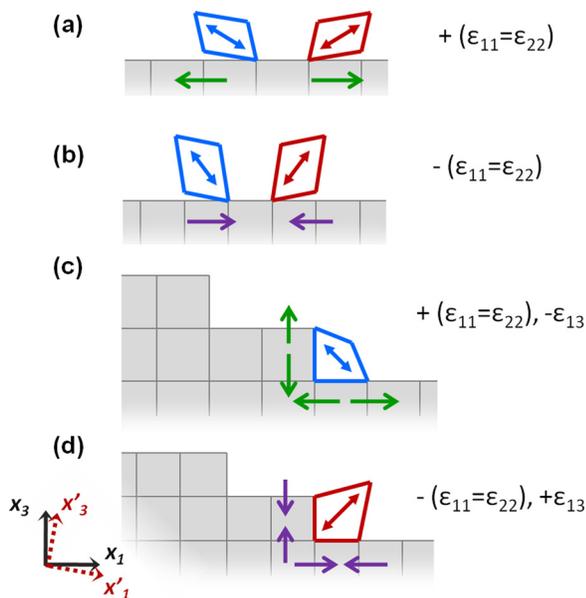
FIG. 3. (Color online) Schematic of ferroelastic variant formation for (a),(b) $(001)_c$-oriented and (c),(d) miscut substrates. For an $(001)_c$-oriented substrate, all four ferroelastic variants are degenerate under both (a) tensile and (b) compressive strain. For the miscut substrate, mismatch strain will be along the global x'_1-x'_2 plane, which in the local system translates to include a shear strain. A tensile strain favors in-plane variants (those tilted towards the global x'_1-x'_2 plane) (c), while a compressive strain favors out-of-plane variants (d).

with compressive strains favoring the out-of-plane variants and tensile strains favoring the in-plane variants.

In conclusion, we use a Ginzburg-Landau-Devonshire phase-field model to describe the evolution of ferroelectric and ferroelastic domain structures $BiFeO_3$ thin films. We find that the domain structures of $BiFeO_3$ thin films are strongly dependent on the combination of orientation and strain. Furthermore, a small degree of miscut is sufficient to cause a degeneracy of favored ferroelectric variants for strong-strain substrates such as $SrTiO_3$, due to the elastic effects from the substrate mismatch. Due to the importance of strain in breaking polarization symmetry in miscut films, we expect that the degree of miscut needed to produce domain non-degeneracy will depend strongly on the magnitude of the misfit strain.

[1] J. Wang, J. B. Neaton, H. Zheng, V. Nagarajan, S. B. Ogale, B. Liu, D. Viehland, V. Vaithyanathan, D. G. Schlom, U. V. Waghmare, N. A. Spaldin, K. M. Rabe, M. Wuttig, and R. Ramesh, Science **299**, 1719 (2003).

[2] T. Zhao, A. Scholl, F. Zavaliche, K. Lee, M. Barry, A. Doran, M. P. Cruz, Y. H. Chu, C. Ederer, N. A. Spaldin, R. R. Das, D. M. Kim, S. H. Baek, C. B. Eom, and R. Ramesh, Nature Mater. **5**, 823 (2006).

[3] N. A. Spaldin and M. Fiebig, Science **309**, 391 (2005).

[4] J. F. Li, J. L. Wang, M. Wuttig, R. Ramesh, N. Wang, B. Ruette, A. P. Pyatakov, A. K. Zvezdin, and D. Viehland, Appl. Phys. Lett. **84**, 5261 (2004).

[5] S. H. Baek, H. W. Jang, C. M. Folkman, Y. L. Li, B. Winchester, J. X. Zhang, Q. He, Y. H. Chu, C. T. Nelson, M. S. Rzchowski, X. Q. Pan, R. Ramesh, L. Q. Chen, and C. B. Eom, Nature Mater. **9**, 309 (2010).

[6] S. K. Streiffer, C. B. Parker, A. E. Romanov, M. J. Lefevre, L. Zhao, J. S. Speck, W. Pompe, C. M. Foster, and G. R. Bai, J. Appl. Phys. **83**, 2742 (1998).

[7] J. W. Park, S. H. Baek, P. Wu, B. Winchester, C. T. Nelson, X. Q. Pan, L. Q. Chen, T. Tybell, and C. B. Eom, Appl. Phys. Lett. **97**, 212904 (2010).

[8] H. W. Jang, D. Ortiz, S. H. Baek, C. M. Folkman, R. R. Das, P. Shafer, Y. Chen, C. T. Nelson, X. Pan, R. Ramesh, and C. B. Eom, Adv. Mater. **21**, 817 (2009).

[9] Y. B. Chen, M. B. Katz, X. Q. Pan, R. R. Das, D. M. Kim, S. H. Baek, and C. B. Eom, Appl. Phys. Lett. **90**, 072907 (2007).

[10] Y. H. Chu, M. P. Cruz, C. H. Yang, L. W. Martin, P. L. Yang, J. X. Zhang, K. Lee, P. Yu, L. Q. Chen, and R. Ramesh, Adv. Mater. **19**, 2662 (2007).

[11] R. R. Das, D. M. Kim, S. H. Baek, C. B. Eom, F. Zavaliche, S. Y. Yang, R. Ramesh, Y. B. Chen, X. Q. Pan, X. Ke, M. S. Rzchowski, and S. K. Streiffer, Appl. Phys. Lett. **88**, 242904 (2006).

[12] F. Zavaliche, S. Y. Yang, T. Zhao, Y. H. Chu, M. P. Cruz, C. B. Eom, and R. Ramesh, Phase Transitions **79**, 991 (2006).

[13] Y. L. Li, S. Y. Hu, and L. Q. Chen, J. Appl. Phys. **97**, 034112 (2005).

[14] Y. L. Li, S. Y. Hu, Z. K. Liu, and L. Q. Chen, Appl. Phys. Lett. **81**, 427 (2002).

[15] Y. L. Li, S. Y. Hu, Z. K. Liu, and L. Q. Chen, Acta Mater. **50**, 395 (2002).

[16] Y. L. Li, L. Q. Chen, G. Asayama, D. G. Schlom, M. A. Zurbuchen, and S. K. Streiffer, J. Appl. Phys. **95**, 6332 (2004).

[17] J. X. Zhang, Y. L. Li, Y. Wang, Z. K. Liu, L. Q. Chen, Y. H. Chu, F. Zavaliche, and R. Ramesh, J. Appl. Phys. **101**, 114105 (2007).

[18] J. X. Zhang, Y. L. Li, S. Choudhury, L. Q. Chen, Y. H. Chu, F. Zavaliche, M. P. Cruz, R. Ramesh, and Q. X. Jia, J. Appl. Phys. **103**, 094111 (2008).

[19] L. Q. Chen and J. Shen, Comput. Phys. Commun. **108**, 147 (1998).

[20] H. W. Jang, D. Ortiz, S. H. Baek, C. M. Folkman, R. R. Das, P. Shafer, Y. Chen, C. T. Nelson, X. Pan, R. Ramesh, and C. B. Eom, Proceedings of the14th US-Japan Seminar on Dielectric and Piezoelectric Materials (14th US-Japan Seminar on Dielectric and Piezoelectric Ceramic Thin Films, Welches, OR, 2009).

[21] The parameters used in the simulations, in SI units (where the temperature T is in K): $\alpha_1 = 4.9(T - 1103) \times 10^5$, $\alpha_{11} = 6.50 \times 10^8$, $\alpha_{12} = 1.0 \times 10^8$, $Q_{11} = 0.032$, $Q_{12} = -0.016$, $Q_{44} = 0.02$, $c_{11} = 3.00 \times 10^{11}$, $c_{12} = 1.62 \times 10^{11}$, $c_{44} = 0.691 \times 10^{11}$.

FIG. 4. (Color online) Domain structures of miscut $BiFeO_3$ simulations under different substrate strains. (a) $\varepsilon'_{11} = \varepsilon'_{22} = -1.5\%$, (b) $\varepsilon'_{11} = \varepsilon'_{22} = -0.0\%$, (c) $\varepsilon'_{11} = \varepsilon'_{22} = +1.5\%$. When the miscut film is sufficiently strained, two ferroelastic variants become favored and the variants line up in a striped domain structure, as seen with compressive strain with r_1/r_4 variants (a), and with tensile strain with r_2/r_3 variants (c). Under weak strain (b), all four variants are degenerate.